Solar Energy Materials & Solar Cells 95 (2011) 3124–3129

Contents lists available at ScienceDirect

Solar Energy Materials & Solar Cells

journal homepage: www.elsevier.com/locate/solmat

Temperature dependence of InGaN/GaN multiple quantum well based high efficiency solar cell

Asghar Asgari [a,b,*], Kh. Khalili [a]

[a] Research Institute for Applied Physics, University of Tabriz, Tabriz 51665-163, Iran
[b] School of Electrical, Electronic and Computer Engineering, The University of Western Australia, Crawley, WA 6009, Australia

ARTICLE INFO

Article history:
Received 31 December 2010
Received in revised form
29 June 2011
Accepted 2 July 2011
Available online 23 July 2011

Keywords:
Multi-quantum well solar cells
Temperature effects
III-nitride materials

ABSTRACT

In this paper, a new p–InGaN multiple quantum well–n solar cell has been investigated. In order to obtain the exact solar cell parameters such as conversion efficiency, the polarization field effects of nitride materials are taken into account. It has been found that the conversion efficiency of the p–i(MQW)–n solar cell is significantly higher than those of normal p–i(bulk)–n solar cells. The optimized conversion efficiency of about 35% is obtained for p–MQW–n solar cells at room temperature. Also, the temperature dependence of open-circuit voltage and short-circuit current and consequently conversion efficiencies of both structures are investigated, and it is observed that the increasing of temperature slightly increases the short-circuit current and decreases the open-circuit voltage and efficiency.

1. Introduction

III-nitride materials, and related nanostructures, have been currently attracting considerable interest for applications in the field of electronics and optoelectronics. The advantages of III-nitride based heterostructures have been achieved because of a large critical breakdown electric field, a large conduction band discontinuity between GaN and Al(In)GaN, and the presence of polarization fields that allow two-dimensional electron gas (2DEG) to be confined at the interface. Also, their direct bandgap in the visible–ultraviolet regions of the electromagnetic spectrum makes them suitable for implementation of devices such as emitters and detectors over a broad spectral region [1,2]. Because of these advantages together with broad absorption spectral coverage (350–1800 nm), high absorption coefficient, and high durability under high-energy particle bombardment for space solar cell application, InGaN/GaN heterostructures have been considered for solar cell application [3–9].

One of the biggest problems in the application of InGaN films is the large mismatch between InN and GaN, resulting in low solubility and phase separation. Therefore the primary challenge in III–V nitride photovoltaics is the reduction of phase separation, as the lower bandgap phase-separated material not only reduces the open-circuit voltage of the solar cell but also enhances recombination, decreasing the photo-generated current. The efficiency of such solar cells can be generally increased by lowering their bandgaps and enhancing absorption for practical applications [2,10].

Usage of quantum wells to enhance solar cell efficiencies has been the subject of a number of studies in recent years mainly by Barnham and co-workers [11,12] at Imperial College. Implementing QWs in solar cells lead to not only the absorbing of additional photons below the band gap energy of the bulk materials, but also determining the absorption edge of the solar cell by the width and depth of QWs [13,14]. Previous studies on single and multiple quantum well solar cells have shown that increase in the short-circuit current (I_{SC}) can be achieved as a result of photo-generation of carriers within the quantum wells and, equally important, the subsequent release of these carriers from the well [15–17]. On the other hand, it has been found that the efficiency improvement of such devices is limited by a reduction in the open-circuit voltage (V_{OC}). It is well known that this reduction also depends on factors other than the band gap of the well material. There has been some controversy over the reasons for MQW solar cell efficiency enhancement, particularly on whether it is associated with the nature and dimension of the well material or it is solely due to enhanced I_{SC} [18,19]. In all investigations, the material quality of the grown MQW structure has been found to be extremely significant. Furthermore it should be taken into account that under significant forward bias voltage and illumination at elevated temperatures, the MQW solar cells exhibited enhanced I_{SC}. In addition they exhibited higher V_{OC} [20].

It has been claimed that the barrier materials determine V_{OC}, while I_{SC} is determined by the well materials. V_{OC} and I_{SC} can be

* Corresponding author at: Research Institute for Applied Physics, University of Tabriz, 29 Bahman Avenue, Tabriz 51665-163, Iran. Tel.: +98 411 339 3005; fax: +98 411 334 7050.
E-mail address: asgari@tabrizu.ac.ir (A. Asgari).

0927-0248/$ - see front matter © 2011 Elsevier B.V. All rights reserved.
doi:10.1016/j.solmat.2011.07.001

independently controlled and optimized. Therefore, the efficiency of multiple quantum well solar cells (MQWSC) can easily exceed that of a single bandgap solar cell [21]. On the other hand, the sun high density wavelengths are limited and to optimize the V_{OC} and I_{SC} in MQWSC, one has to focus on the whole structure. In this work, the III-nitride materials based p–MQW–n and reference p–i–n solar cells with different structures are investigated theoretically and the temperature dependence of solar cells parameters is obtained.

2. Theoretical model

The solar radiation intensity above the atmosphere reaches 1353 W m^{-2}, with a spectrum centered near 495 nm wavelength. Therefore, at the ground level, this spectral density is reduced to only near 1000 W m^{-2}. In order to evaluate the atmosphere effect on incident solar radiation, the air mass defined by AM$=1/\cos\gamma$ was used, where γ represents the angle between the sun and the vertical. AM0 represents the conditions outside the atmosphere. At the ground level, it is more adequate to use AM1.5 [22].

2.1. p–i(bulk)–n solar cell

To model the device and optimize its parameters, a bulk GaN/$In_xGa_{1-x}N$/GaN p–i–n solar cell with an i-region of 220 nm thickness has been considered [2]. By considering only free electron–hole band to band transitions for the calculation, the absorption coefficient for free carriers can be written as

$$\alpha(\omega)=\alpha_0^D\frac{\hbar\omega}{E_0}\left(\frac{\hbar\omega-E_g-E_0^{(D)}}{E_0}\right)^{D-2/2}\Theta(\hbar\omega-E_g-E_0^{(D)})A(\omega) \tag{1}$$

where $\Theta(x)$ is the Heaviside unit-step function, $\alpha_0^D=4\pi^2|d_{cv}|^2/\hbar n_b c 1/(2\pi a_0)^D\Omega_D 1/L_c^{3-D}$, $\hbar\omega$ is the photon energy, and $A(\omega)=1-f_e(\omega)-f_h(\omega)$, $E_0=h^2/(2m_r a_0^2)$, and $a_0=h^2\varepsilon_0/(e^2 m_r)$ are the scaling parameters. In the calculation we assumed the structure to be an unexcited material, where $f_e(\omega)=f_h(\omega)=0$, i.e., $A(\omega)=1$ [23]. The current density of conventional p–i–n solar cell as a function of applied voltage (V) can be expressed by the well-known Shockly equation for ideal diode:

$$J(V)=J_0[\exp(qV/k_BT)-1]-J_G+J_R \tag{2}$$

where the reverse saturation current J_0 is

$$J_0=qn_{iB}^2A\left(\frac{D_p}{L_pN_D}+\frac{D_n}{L_nN_A}\right) \tag{3}$$

where A is the junction area, n_{iB} is the equilibrium intrinsic concentration in i-region, D_n and D_p denote the electron and hole diffusion coefficients, and L_n and L_p are the electron and hole diffusion lengths, respectively, k_B is the Boltzman constant, T is the absolute temperature, q is the electron charge, and J_G and J_R are the superposed current densities corresponding to carrier generation and recombination in the intrinsic region, respectivily [24,25]. The generation current densities can be written as

$$J_G=qw[G_{Bopt}+G_{Bth}] \tag{4}$$

where w is the intrinsic region width, and G_{Bopt} and G_{Bth} are the average optical and thermal generation rate, respectively, throughout the intrinsic region.

The recombination current is given by

$$J_R=qwR_B=qwB_Bn_{iB}^2\exp(qV/k_BT) \tag{5}$$

where R_B is the average recombination rate in the intrinsic region and B_B is the barrier recombination coefficient. Substituting Eqs. (4) and (5) in Eq. (2) and noting that $G_{Bth}=B_Bn_{iB}^2$, one can get $J(V)$ for the ideal p–i(bulk)–n solar cell:

$$J_B(V)=J_0(1+\beta)[\exp(qV/k_BT)-1]-qwG_{\mathrm{Bopt}} \tag{6}$$

where the ratio of the current required to feed radiative recombination in the intrinsic region at equilibrium to the usual reverse drift current resulting from minority carrier extraction is [11]

$$\beta=\frac{qwB_Bn_{iB}^2}{J_0} \tag{7}$$

The short-circuit current and open-circuit voltage, respectively, for the bulk solar cell are finally

$$J_{scB}=-qwG_{Bopt} \tag{8}$$

$$V_{ocB}=\frac{k_BT}{q}\ln\left(\frac{|J_{scB}|+J_0(1+\beta)}{J_0(1+\beta)}\right) \tag{9}$$

These expressions differ from the ideal model only by a reduction of the open circuit voltage by an amount of $(k_BT/q)\ln(1+\beta)$. This reduction will typically be of inconsequential magnitude, but it has been included for purposes of comparison with the quantum well cell model that will be developed [11]. The efficiency of the solar cell is given by

$$\eta=\frac{V_mJ_m}{P_{in}}\times 100\% \tag{10}$$

where $P_{in}=1000$ W m^{-2} is the input power from the sunlight for 1-sun under AM1.5 condition. Here J_m is the current corresponding to the maximum power output, which is obtained by derivation of $P=JV$ with respect to current density J and setting $\partial P/\partial J=0$. V_m is obtained by solving the following equation using the iteration procedure:

$$\exp(V_m/V_T)\left[1+\frac{V_m}{V_T}\right]=\exp(V_{oc}/V_T) \tag{11}$$

where $V_T=k_BT/q$ is the thermal voltage. Another important solar cell parameter is the fill factor (FF), which measures the squareness of the photo-J–V curve, defined by [26]

$$FF=\frac{V_mJ_m}{V_{oc}J_{sc}} \tag{12}$$

2.2. p–(MQW)–n solar cell

The quantum well solar cell (QWSC) consists of a multiple quantum well structure in the intrinsic region of a p–i–n cell [24]. The MQW structure introduced for the model is constructed by a InGaN with band gap energy of E_B for the barriers and InGaN with lower indium molar fraction and narrow bandgap of E_A ($E_A<E_B$) for the wells, which is schematically shown in Fig. 1.

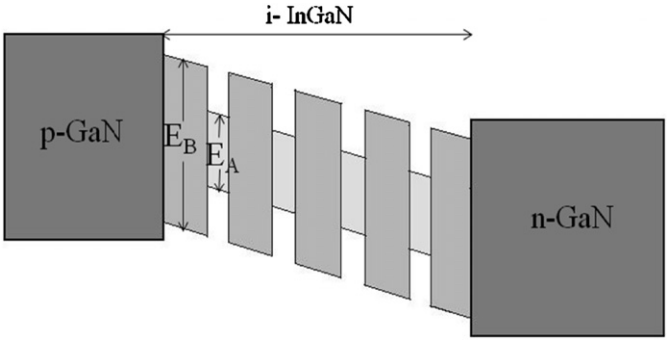

Fig. 1. Schematic profile of p–i(MQW)–n solar cell.

The optical absorption spectrum of multiple quantum well material in an electric field can be written as

$$\alpha(\hbar\omega,F)=M_{cv}^2 q_{ex} L(\hbar\omega,E_{cv}^{1,1}(F)-E_b)+\int_{E_{cv}^{1,1}(F)}^{\infty} M_{cv}^2 N q_{con} K(E',E_{cv}^{1,1}(F)) L(\hbar\omega,E')\,dE' \tag{13}$$

where the Lorentzian function is defined as

$$L(\hbar\omega,E)=\frac{\Gamma_{hom}^2}{2\pi[(h\omega,E)^2+\Gamma_{hom}^2]} \tag{14}$$

and $E_{cv}^{1,1}$ is the separation between the $n=l$ valence and conduction subbands, E_b is the exciton binding energy, Γ_{hom} is the full width at half maximum (FWHM) of the homogeneous broadening caused by phonon interaction and tunneling through barriers, q_{ex} and q_{con} are the oscillator strengths of the excitonic and band to band transitions, respectively, N is the joint density of states between valence and conduction bands, M_{cv} is the electron–hole overlap integral, and K is continuum shape of the Sommerfeld factor. It should be mentioned that the assumption of Elliot's theory regarding the absorption that is used in this manuscript is: (i) a continuum of transitions between free particle states and (ii) excitonic transitions. Also, in excitonic transition, only the first exciton state, 1*S*, is considered [27].

As the studied MQW structure is III-nitride materials, one has to take into account the effects of spontaneous and piezoelectric polarization to achieve the accurate results of modeled solar cell. The electric field inside the generic *j*th layer (either QW or barrier) is given by

$$E_j=\frac{\sum_k l_k P_k/\varepsilon-P_j\sum_k l_k/\varepsilon_k}{\varepsilon_j\sum_k l_k/\varepsilon_k} \tag{15}$$

where P_j and ε_j are the total polarization (spontaneous and piezoelectric) and dielectric constant in layer *j*, respectively, and l_j is thickness of *j*th layer [28].

The current–voltage characteristics for MQW solar cell using the Shockly equation and in combination with generation and recombination currents in both wells and barriers can be written as

$$J_{QW}(V)=J_0[1+r_R\beta][\exp(qV/k_BT)-1]-qw[f_w G_{Wopt}+(1-f_w)G_{Bopt}] \tag{16}$$

where

$$r_R=1+f_w[\gamma_B\gamma_{DOS}^2\exp(\Delta E/k_BT)-1] \tag{17}$$

and $\gamma_B=B_W/B_B$, $\gamma_{DOS}=g_W/g_B$ (where g_W and g_B are the effective volume densities of states for the wells and barriers, respectively), and $\Delta E=E_B-E_A$. In the unity quantum efficiency limit, where all incident photons with energies above the lowest bandgap in the cell are absorbed in the intrinsic region, the short-circuit current can be expressed as

$$J_{scB}=-qwG_{Bopt}=-q\Phi_B, \tag{18}$$

$$J_{scQW}=-qw[f_W G_{Wopt}+(1-f_W)G_{Bopt}]=-q\Phi_A, \tag{19}$$

where Φ_B and Φ_A are the flux of incident photons absorbed by barrier and well materials, respectively [11]. The flux of incident light as a function of wavelength in AM1.5 spectrum is given by

$$\Phi(\lambda)=3.5\times10^{21}\lambda^{-4}[\exp(hc/kT_s\lambda)]^{-1}\ \text{photon}/\mu\text{m s cm}^2, \tag{20}$$

where h and c are the Plank constant and light velocity in vacuum, respectively, and $T_s=5670$ K [29]. Therefore, the $J(v)$ relations become

$$J_B(V)=J_0(1+\beta)[\exp(qV/k_BT)-1]-qw\Phi_B. \tag{21}$$

For the reference solar cell, these yield an open-circuit voltage and short-circuit current of

$$J_{scB}=-q\Phi_B, \tag{22a}$$

$$V_{ocB}=\frac{k_BT}{q}\ln\left(\frac{q\Phi_B+J_0(1+\beta)}{J_0(1+\beta)}\right) \tag{22b}$$

$$J_{QW}(V)=J_0(1+r_R\beta)[\exp(qV/k_BT)-1]-q\Phi_A \tag{23}$$

corresponding to [11]

$$J_{scQW}=-q\Phi_A, \tag{24a}$$

$$V_{scQW}=\frac{k_BT}{q}\ln\left(\frac{q\Phi_A+J_0(1+r_R\beta)}{J_0(1+r_R\beta)}\right). \tag{24b}$$

3. Results and discussion

3.1. p–i(bulk)–n solar cell

To model the p–i–n (p–MQW–n) solar cells, a structure that includes a p-GaN layer with 100 nm thickness, doping values for the p- and n-region of 2×10^{17} and 4×10^{18} cm^{-3}, respectively, and the minority carrier lifetime for all materials of 2 ns have been assumed, while the hole and electron mobilities are fixed at 10 and 400 cm^2/V s, respectively. The other physical parameters of the material and structures used in the calculation are presented in Tables 1 and 2.

To find the ideal composion for the i-region of the p–i–n solar cells, the absorption coefficient of reference p–i–n solar cell as a function of Indium mole fraction has been calculated. The calculation results show that the increasing of In mole fraction increases the absorption coefficient of p–i(bulk)–n solar cells and shifts it to long wavelengths. For structures with In mole fraction of $x>0.3$ the solar cell absorbs light of wavelength $\lambda=495$ nm, which has the highest intensity in sunlight (Fig. 2). So the structure with In mole fraction of 0.3, i.e. $In_{0.3}Ga_{0.7}N$, is used as the i-region material. The current–voltage characteristics for the p–i–n structure with $In_{0.3}Ga_{0.7}N$ in i-region are shown in Fig. 3, where $J_{sc}=1.5$ mA/cm^2, $V_{oc}=1.86$ V, and $\eta=2.5\%$ are obtained.

The *I–V* curves for different solar cells with different i-region structures that include different In mole fractions are investigated. As shown in Fig. 4 with decreasing Indium mole fraction and consequently narrowing bandgap, the open-circuit voltage decreases and the short-circuit current increases due to the increasing of carrier generation.

Table 1
The InGaN characterization parameters.

Parameters of $In_xGa_{1-x}N$ (unit)	Value	Reference
Bandgap (eV)	$0.7x+3.4(1-x)-1.43x(1-x)$	[30]
m_e (m_0)	$0.13-0.02x$	[1]
m_{hh} (m_0)	$1.52-0.11x$	[1]
Lattice constant a (Å)	$3.19+0.35x$	[1]
Dielectric constant ε (ε_0)	$10.4+4.9x$	[31]
ϵ-In-plane strain	$2\left(\frac{a_{GaN}-a_{In_xGa_{1-x}N}}{a_{In_xGa_{1-x}N}}\right)$	[31]

Table 2
Piezoelectric constant, elastic constant and spontaneous polarization in nitride-based binaries.

Parameters (unit)	GaN	InN	Reference
e_{33} (C m^{-2})	0.73	0.97	[32]
e_{31} (C m^{-2})	−0.49	−0.57	[32]
c_{33} (GPa)	405	224	[32]
c_{31} (GPa)	103	92	[32]
p_{sp} (C m^{-2})	−0.029	−0.032	[32]
$e_{31}-(c_{31}/c_{33})e_{33}$	−0.68	−0.97	[32]

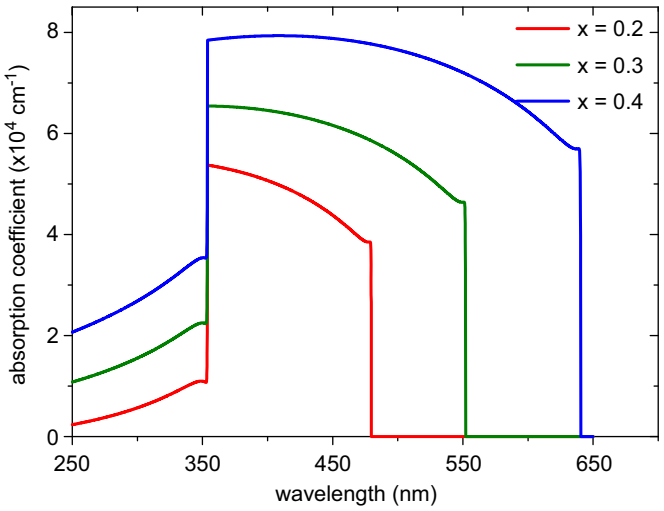

Fig. 2. Absorption coefficient for bulk p–i(InGaN)–n solar cell with different Indium molar fractions.

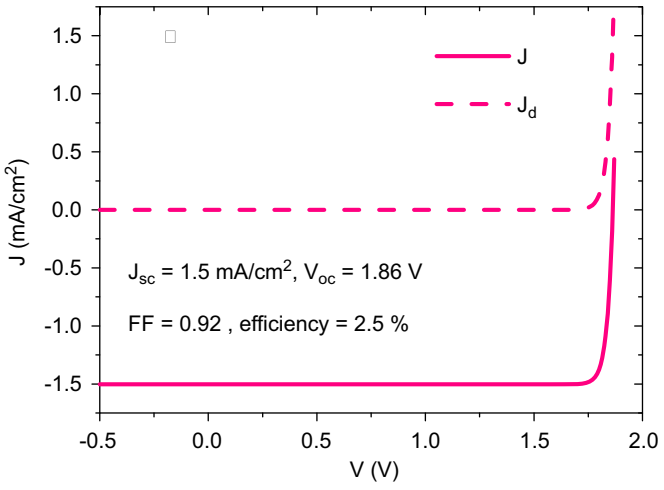

Fig. 3. Current–voltage characteristics and input power for bulk p–i($In_{0.3}Ga_{0.7}N$)–n solar cell.

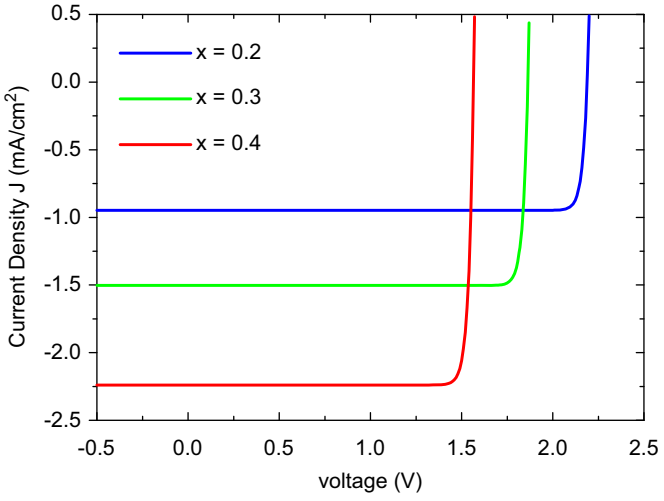

Fig. 4. Current–voltage characteristics of p–i–n solar cells for different Indium mole fractions in the i-region.

The effects of temperature on the p–i(bulk)–n solar cell parameters such as open-circuit voltage, short-circuit current, and conversion efficiency are calculated and expressed in Fig. 5.

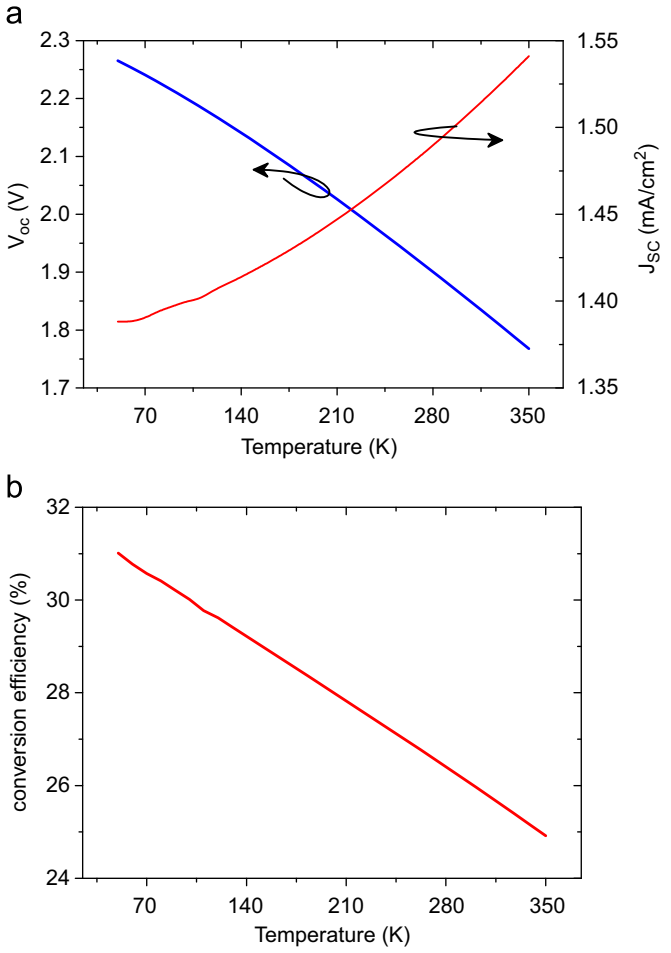

Fig. 5. Temperature dependences of (a) V_{oc} and J_{sc} (b) conversion efficiency in the bulk p–i($In_{0.3}Ga_{0.7}N$)–n solar cell.

As depicted in the figure, with increasing temperature the open-circuit voltage decreases due to the bandgap narrowing, and short-circuit current increases. The decreasing rate of the voltage is more than the current increasing rate, so as a result with increasing of temperature the conversion efficiency decreases. The reason is that the photo-generated carriers with lower energy materials have a larger probability to recombination when the temperature becomes higher.

3.2. *p–(MQW)–n solar cell*

The sample used in the modeling is the p–i–n solar cells with an $In_xGa_{1-x}N/In_yGa_{1-y}N$ MQW structure within the i-region. The p- and n-regions are based on GaN. The donor and acceptor concentrations in the n- and p-region materials are assumed to be the same and equal to $N=0.1\times10^{18}$ cm^{-3}. Initially, the quantum well subband energy and related wavefunctions of the electron and hole have been calculated using the numerical transfer matrix method (TMM). Also in the calculation only the first subband transition (with uncoupled heavy and light hole states) has been considered. Using these wavefunctions, the absorption spectrum of the MQW structure has been determined. It should be notified that the calculated built in polarization field for the structures is about $\sim10^8$ V/m.

The absorption coefficient versus wavelength for the GaN/InGaN/GaN p–MQW–n solar cell that consists of 25 wells with different In mole fractions and various thicknesses, 26 barriers with $x_b=0.1$, and barrier thickness of 5 nm is calculated and

depicted in Fig. 6. Fig. 6a shows the absorption coefficient for the structures with the well thickness of 3 nm and Indium mole fraction in the well of 0.3, 0.35, and 0.4. Also, Fig. 6b indicates the absorption coefficient for the structures with the well thickness of 2, 2.5, and 3 nm and Indium mole fraction in the well of 0.3. As depicted in the figures, with increasing well width and Indium mole fraction in the well material, the absorption coefficient shifts to long wavelengths. Also with increasing well width, the absorption coefficient decreases.

Knowing the absorption coefficient, the voltage, and the current, the conversion efficiency for the p–MQWSC–n solar cells can be calculated. The conversion efficiency of the cells that consist of the MQW structure with 25 wells and well thickness of 1 nm, also 26 barriers with $x_b=0.1$, and barrier thickness of 5 nm as a function of Indium mole fraction in the well is calculated and shown in Fig. 7. As depicted in the figure, the optimum conversion efficiency is obtained for the solar cell with Indium mole fraction of $x_w=0.63$ in the wells.

The current–voltage characteristics of the optimized device are shown in Fig. 8, where the dashed curve denotes the dark current density. At room temperature we attained $J_{sc}=38.04$ mA/cm^2, $V_{oc}=1.03$ V, and $\eta=35\%$ (regardless of loss factors) for the proposed MQWSC structure under AM1.5 condition, which

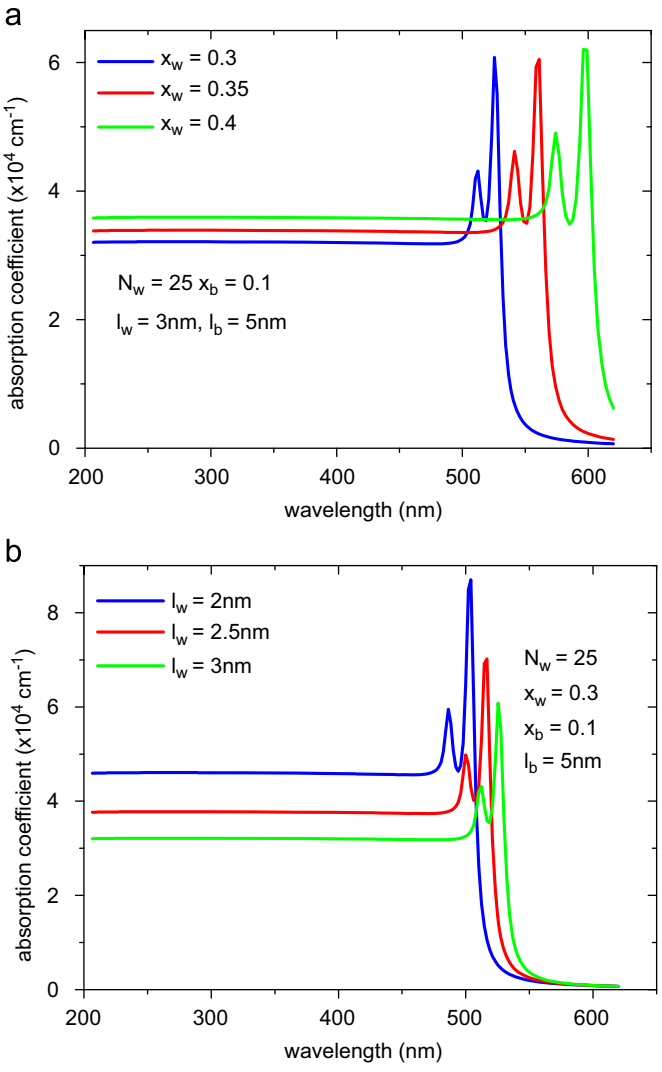

Fig. 6. Absorption coefficient for P–i(MQW)–n solar cell of $In_xGa_{1-x}N$ with (a) different Indium fractions in the well and (b) different well thicknesses.

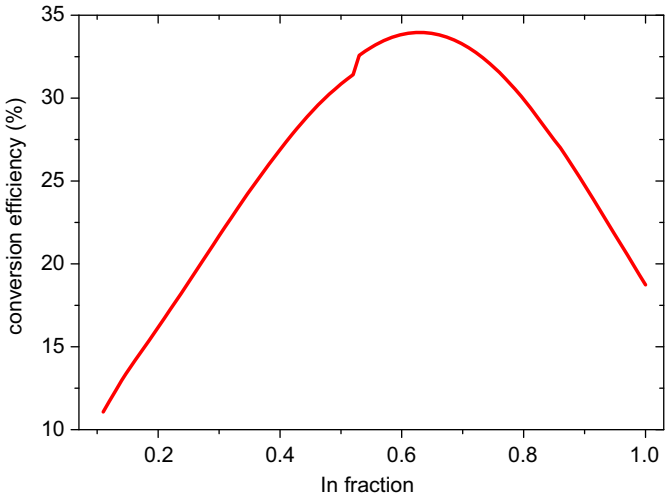

Fig. 7. Conversion efficiency of MQWSC as a function of Indium molar fraction in the well material.

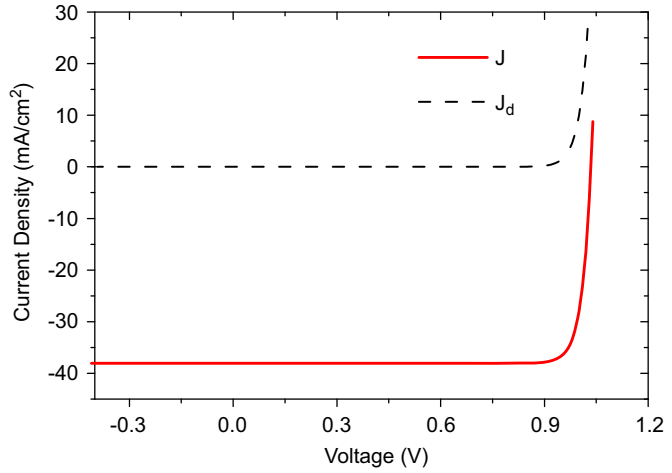

Fig. 8. Current–voltage characteristics for p–i–n solar cell with a MQW structure in intrinsic region.

is comparable to the optimized parameters obtained in the model of Prazmowska and Korbutowicz [14].

Consequently, the temperature dependences of the open-circuit voltage, short-circuit current, and conversion efficiency of the optimized p–MQWSC–n solar cell structure are calculated and shown in Figs. 9. and 10. As depicted in the figures, with increasing temperature the open-circuit voltage decreases and the short-circuit current increases. The decreasing rate of voltage is more than the current increasing rate; thus with increasing temperature the conversion efficiency decreases. The conversion efficiency reaches 35% at room temperature. This is in good agreement with the experimental results obtained by Jeng et al. [21].

A comparison of conversion efficiency between p–i(bulk)–n and p–MQW–n solar cells in Figs. 5 and 10 shows that the conversion efficiency in p–MQW–n solar cells can exceed than that of single bandgap solar cell.

4. Conclusion

The current density versus voltage for two p–i–n (p–MQW–n) solar cell structures has been investigated and it has been observed that short-current density and consequently conversion

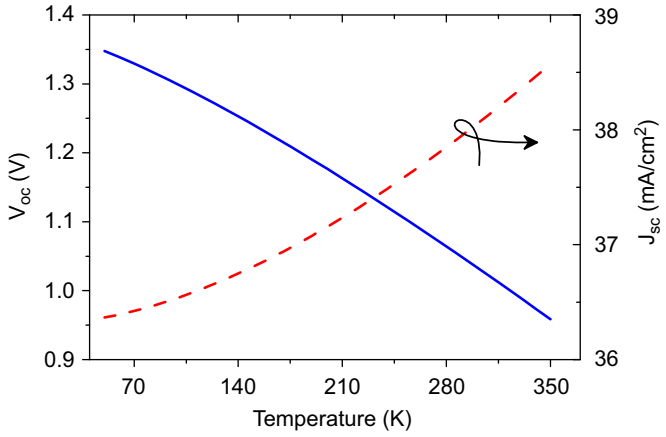

Fig. 9. Open-circuit voltage and short-circuit current for p–i(MQW)–n solar cells as a function of temperature.

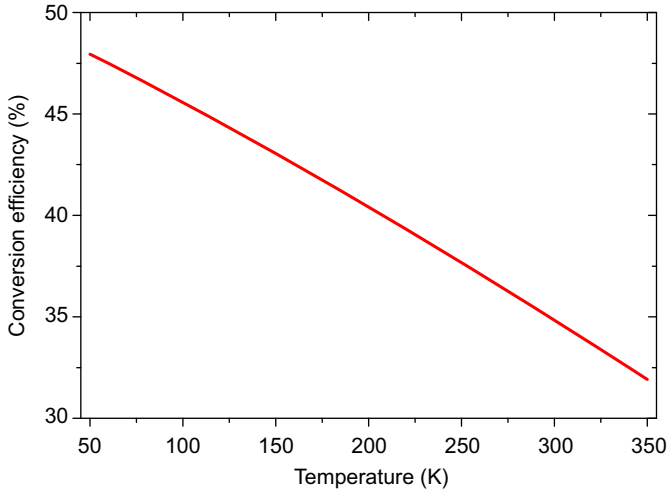

Fig. 10. Conversion efficiency of p–i(MQW)–n solar cells as a function of temperature.

efficiency of MQWSC is significantly larger than that of the reference p–i–n solar cell. The maximum quantum efficiency near 35% (regardless of loss factors) under 1-sun AM1.5 condition was obtained in InGaN multiple quantum well solar cells at room temperature. Calculations of temperature dependences for both MQWSC and reference p–i–n solar cell that with increasing temperature, the conversion efficiency decreases. This is believed to be due to the low QW energy barrier and recombination effects in the MQWSCs.

References

[1] A. Asgari, S. Razi, High performances III-nitride quantum dot infrared photodetector operating at room temperature, Opt. Express 18 (2010) 14604–14615.

[2] O. Jani, I. Ferguson, C. Honsberg, S. Kurtz, Design and characterization of GaN/InGaN solar cell, Appl. Phys. Lett. 91 (2007) 132117 (pp. 3).

[3] F.K. Yam, Z. Hassan, InGaN: an overview of the growth kinetics, physical properties and emission mechanisms, Superlattices and Microstructure 43 (2008) 1–23.

[4] S.M. Sze, Ng.K. Kowk, Physics of Semiconductor Devices, 3rd Edition, Wiley, New York, 2006.

[5] L. Hsu, W. Walukiewicz, Modeling of InGaN/Si tandem solar cells, J. Appl. Phys. 104 (2008) 024507 (pp. 7).

[6] Elison Matioli, Carl Neufeld, Michael Iza, Samantha C. Cruz, Ali A. Al-Heji, Xu Chen, Robert M. Farrell, Stacia Keller, Steven Den Baars, Umesh Mishra, Shuji Nakamura, James Speck, Claude Weisbuch, High internal and external quantum efficiency InGaN/GaN solar cells, Appl. Phys. Lett. 98 (2011) 021102 (pp. 3).

[7] K.Y. Lai, G.J. Lin, Y.-L. Lai, Y.F. Chen, J.H. He, Effect of indium fluctuation on the photovoltaic characteristics of InGaN/GaN multiple quantum well solar cells, Appl. Phys. Lett. 96 (2010) 081103 (pp. 3).

[8] Ray-Hua Horng, Mu-Tao Chu, Hung-Ruei Chen, Wen-Yih Liao, Ming-Hsien Wu, Kuo-Feng Chen, Dong-Sing Wuu, Improved conversion efficiency of textured InGaN solar cells with interdigitated imbedded electrodes, IEEE Electron. Device. Lett. 31 (2010) 585–587.

[9] R. Dahal, J. Li, K. Aryal, J.Y. Lin, H.X. Jiang, InGaN/GaN multiple quantum well concentrator solar cells, Appl. Phys. Lett. 97 (2010) 073115 (pp. 3).

[10] R. Dahal, B. Pantha, J. Li, J.Y. Lin, H.X. Jiang, InGaN/GaN multiple quantum well solar cells with long operation wavelengths, Appl. Phys. Lett. 94 (2009) 063505 (pp. 3).

[11] N.G. Anderson, Ideal theory of quantum well solar cell, J. Appl. Phys. 78 (1995) 1850–1861.

[12] K.W.J. Barnham, I. Ballard, J.P. Connolly, N.J. Ekins-Daukes, B.G. Kluftinger, J. Nelson, C. Rohr, Quantum well solar cell, Physica E 14 (2002) 27–36.

[13] A. Asgari, Kh. Khalili, E. Ahmadi, S. Ahmadi-Kandjani, High efficiency iii-nitride based p-i-n solar cell, in: Proceeding of second International Conference on Nuclear and Renewable Energy Resources, Turkey, (2010) pp. 334–339.

[14] J. Prazmowska, R. Korbutowicz, Optimization of multi quantum well solar cell, Opt. Appl. XXXV (2005) 619–628.

[15] J. Nelson, K.W.J. Barnham, J.P. Connolly, G. Haarpaintner, C. Button, J. Roberts, Quantum well solar cell dark current, in: Proceedings of the 12th European Photovoltaic Solar Energy Conference, (1994) pp. 1370–1373.

[16] J. Barnes, T. Ali, K.W.J. Barnham, J. Nelson, E.S.M. Tsui, J. Roberts, M.A. Pate, S.S. Dosanjh, Gallium arsenide/indium gallium arsenide multi-quantum well solar cells, in: Proceedings of the 12th European Photovoltaic Solar Energy Conference, (1994) pp. 1374–1377.

[17] D.E. Ashenford, A.W. Dweydari, D. Sands, C.G. Scott, M. Yousaf, E. Aperathitis, Z. Hatzopoulos, P. Panayotatos, Investigation of p-i-n solar cell efficiency enhancement by use of MQW structures in the i-region, J. Cryst. Growth. 159 (1996) 920–924.

[18] R. Corkish, M. Green, Recombination of carriers in quantum well solar cells, in: Proceedings of the 23rd IEEE Photovoltaic Specialists Conference, (1993) pp. 675–680.

[19] N.G. Anderson, Ideal theory of quantum well solar cells, J. Appl. Phys. 78 (1995) 1850–1861.

[20] E. Aperathitis, A.C. Varonides, C.G. Scott, D. San, V. Foukaraki, M. Androulidaki, Z. Hatzopoulos, P. Panayotatos, Temperature dependence of photocurrent components on enhanced performance GaAs/AlGaAs multiple quantum well solar cells, Sol. Energy Mater. Sol. Cells 70 (2001) 49–69.

[21] M.J. Jeng, Yu.L. Lee, L.B. Chang, Temperature dependences of $In_xGa_{1-x}N$ multiple quantum well solar cells, J. Phys. D: Appl. Phys. 42 (2009) 105101 (pp. 6).

[22] M. Anani, C. Mathieu, M. Khadraoui, Z. Chama, High-grade efficiency III-nitrides semiconductor solar cell, Microelectronics Journal 40 (2009) 427–434.

[23] H. Haug, S.W. Koch, Quantum Theory of the Optical and Electronic Properties of Semiconductors, 4th edition, World Scientific, World Scientific Publishing Co. Pte. Ltd., Singapore, 2004.

[24] J.C. Rimada, L. Hernandez, Modeling of ideal AlGaAs quantum well solar cell, Microelectronics Journal 32 (2001) 719–723.

[25] S.Li. Sheng, Semi Conductor Physical Electronics, Springer Science & Business Media, LLC, Springer, New York, USA, 2006.

[26] W.J. Aziz, K. Ibrahim, Simulation model of multi-junction $In_xGa_{1-x}N$ solar cell, Int. J. Nanoelectron. Mater. 3 (2010) 43–52.

[27] P.J. Stevens, M. Whitehead, G. Parry, K. Woodbridge, Computer modeling of electric field dependent absorption spectrum of multiple quantum well material, IEEE J. Quantum Electron. 24 (1988) 2007–2016.

[28] F. Bernardini, V. Fiorentini, Spontaneous versus piezoelectric polarization in III–V nitrides: conceptual aspects and practical consequences, Phys. Stat. Sol. (b) 216 (1999) 391–398.

[29] N. Es'haghi Gorji, H. Movla, F. Sohrabi, A. Hosseinpour, M. Rezaei, H. Babaei, The effects of recombination lifetime on efficiency and *J–V* characteristics of $In_xGa_{1-x}N$/GaN quantum dot intermediate solar cell, Physica E 42 (2010) 2353–2357.

[30] J. Wu, W. Walukiewicz, K.M. Yu, W.J. Ager, E.E. Haller, H. Lu, W.J. Schaff, Small band gap bowing in $In_xGa_{1-x}N$ alloys, Appl. Phys. Lett. 80 (2002) 4741 (pp. 3).

[31] H. Morkor, Handbook of Nitride Semiconductors and Devices: GaN-Based Optical and Electronic Devises, vol. 3, Wiley-VCH Verlag GmbH & Co. KGaA, Weinheim, Germany, 2009.

[32] F. Bernardini, V. Fiorentini, D. Vanderbit, Spontaneous polarization and piezoelectric constants of III-V nitrides, Phys. Rev. B 56 (1997) 10024–10027.